Developmental Biology 328 (2009) 422–433

Contents lists available at ScienceDirect

Developmental Biology

journal homepage: www.elsevier.com/developmentalbiology

Origins and control of the differentiation of inhibitory interneurons and glia in the cerebellum

Piercesare Grimaldi [a,b,1], Carlos Parras [c], François Guillemot [d], Ferdinando Rossi [b], Marion Wassef [a,*]

[a] CNRS UMR 8542, Biology Department, Ecole Normale Supérieure, 46 Rue d'Ulm, 75005 Paris, France
[b] Department of Neuroscience and "Rita Levi Montalcini Centre for Brain Repair", National Institute of Neuroscience, University of Turin, I-10125 Turin, Italy
[c] INSERM U711, Hôpital de la Pitié-Salpêtrière, 47 Bd de l'Hôpital, 75651 Paris, France
[d] National Institute for Medical Research, The Ridgeway, Mill Hill, NW71AA London, UK

ARTICLE INFO

Article history:
Received for publication 5 November 2008
Revised 8 January 2009
Accepted 1 February 2009
Available online 13 February 2009

Keywords:
Cerebellum development
GABAergic interneuron
Oligodendrocyte
Astrocyte
Ascl1
Differentiation
Specification

ABSTRACT

Cerebellar GABAergic interneurons and glia originate from progenitors that delaminate from the ventricular neuroepithelium and proliferate in the prospective white matter. Even though this population of progenitor cells is multipotent as a whole, clonal analysis indicates that different lineages are already separated during postnatal development and little is known about the mechanisms that regulate the specification and differentiation of these cerebellar types at earlier stages. Here, we investigate the role of *Ascl1* in the development of inhibitory interneurons and glial cells in the cerebellum. This gene is expressed by maturing oligodendrocytes and GABAergic interneurons and is required for the production of appropriate quantities of these cells, which are severely reduced in *Ascl1*$^{-/-}$ mouse cerebella. Nevertheless, the two lineages are not related and the majority of oligodendrocytes populating the developing cerebellum actually derive from extracerebellar sources. Targeted electroporation of *Ascl1*-expression vectors to ventricular neuroepithelium progenitors enhances the production of interneurons and completely suppresses astrocytic differentiation, whereas loss of *Ascl1* function has opposite effects on both cell types. Our results indicate that *Ascl1* directs ventricular neuroepithelium progenitors towards inhibitory interneuron fate and restricts their ability to differentiate along the astroglial lineage.

Introduction

In several CNS regions, proper development of glial and inhibitory interneuron lineages depends upon the action of the bHLH transcription factor Ascl1 (also called Mash1). Loss of *Ascl1* function provokes a drastic reduction of GABAergic interneurons and oligodendrocytes (Battiste et al., 2007; Casarosa et al., 1999; Fode et al., 2000; Miyoshi et al., 2004; Mizuguchi et al., 2006; Parras et al., 2007; Wildner et al., 2006), and an excessive production of astrocytes (Nieto and Guillemot, 2001), but the underlying mechanism of action in not well understood. *Ascl1* can regulate proliferation and cell cycle exit (Casarosa et al., 1999; Lo et al., 1997), but can also bias the phenotypic choices of progenitor cells (Fode et al., 2000; Lo et al., 2002; Parras et al., 2002; Sugimori et al., 2007). At a later stage, in the telencephalic subventricular zone it is supposed to shift the fate of multipotent progenitors from interneuron to oligodendroglial identities in a cell non-autonomous way, through repression of the Dlx1/2 genes mediated by notch signalling (Petryniak et al., 2007), whereas in the dorsal telencephalon it can promote neurogenesis at the expenses of astrocyte generation (Nieto and Guillemot, 2001).

Here, we investigate the role of *Ascl1* in the differentiation of GABAergic interneurons and glia of the cerebellum. These lineages originate from progenitors that proliferate in the prospective white matter (WM, Milosevic and Goldman, 2004; Zhang and Goldman, 1996a). Although these cells have wide developmental potentialities (Carletti et al., 2002, 2008; Jankovski et al., 1996; Leto et al., 2006; Zhang and Goldman, 1996a, 1996b), clonal analysis *in vitro* suggests that the majority of them are restricted to neuronal or glial phenotypes (Milosevic and Goldman, 2002, 2004). On the other hand, a multipotent stem cell that could give rise to different cerebellar types other than glutamatergic neurons has been isolated from Math1-negative progenitors in the postnatal cerebellar parenchyma (Lee et al., 2005). While distinct lineages appear to be present in the WM, little is known about earlier phases of development in the ventricular zone (VZ), the presumptive site of origin of these precursors (Hoshino et al., 2005). In particular, it remains uncertain whether they derive from distinct progenitor pools or germinal sites and what the role of proneural genes is in the specification of these cerebellar phenotypes.

* Corresponding author. CNRS/ENS UMR 8542, groupe Régionalisation Nerveuse, Ecole Normale Supérieure, 46, rue d'Ulm, 75230 Paris Cedex 05, France. Fax: +33 1 44 32 23 23.
E-mail address: wassef@biologie.ens.fr (M. Wassef).
[1] Current address: Division of Biology, California Institute of Technology, MC 114-96, 1200 E California Blvd., Pasadena, CA 91125, USA.

0012-1606/$ – see front matter © 2009 Elsevier Inc. All rights reserved.
doi:10.1016/j.ydbio.2009.02.008

We show here that *Ascl1* ablation causes a severe reduction of inhibitory interneurons and oligodendrocytes and increases the generation of astrocytes. Fate mapping of cerebellar VZ progenitors reveals that while astrocytes and GABAergic interneurons originate from this germinal layer, the majority of oligodendrocytes derive from extracerebellar territories. *Ascl1* overexpression in the VZ promotes the differentiation of progenitors to interneuron fate and suppresses the astrocytic one. Together, these data demonstrate that in the cerebellum *Ascl1* is not implicated in the switch between oligodendrocytes and interneurons, but in the fate choice along the interneuron and astrocytic lineages.

Materials and methods

Animals and surgical procedures

The care and use of experimental animals followed the French and Italian laws on the care and use of experimental animals, in accordance with the ECC directive (86/609/EEC). *Ascl1*$^{-/-}$ mutant mice were described previously (Fode et al., 2000). The *Pax2*^{GFP} transgenic mouse line was a gift from M. Busslinger (Vienna Biocentre, Vienna, Austria; Pfeffer et al., 2002). *Ascl1*$^{-/-}$ animals were genotyped by PCR as described (Parras et al., 2002). *Ascl1::GFP* from Gensat (Gong et al., 2003), βactin-GFP transgenic mice (GFPU line, Hadjantonakis et al., 1998) and *Pax2*^{GFP} transgenic animals were typed by UV illumination. Midday of vaginal plug detection was considered as embryonic day 0.5 (E0.5). Surgical procedures were performed under deep general anaesthesia obtained by intraperitoneal injection of a mixture of ketamine (100 mg/kg; Ketavet; Bayer) and xylazine (5 mg/kg; Rompun; Bayer) or by ice-chilling for new-born postnatal (P) mice. Pregnant mice were killed with CO_2 before embryo extraction.

The grafts of embryonic cerebella to postnatal recipient mice were performed as described in Cohen-Tannoudji et al. (1994). Since *Ascl1*$^{-/-}$ mice are not viable after birth, to study their mature cerebellar phenotype, cerebellar primordia from E15.5 *Ascl1*$^{-/-}$ and wild type animals ($N=14$ for each group) of the same litter were dissected in phosphate-buffered saline (PBS, with 0.6% glucose and 0.2% penicillin-streptomycin) and grafted to the telencephalon of P2 Swiss mice, which were allowed to survive for 1 month after surgery. To assess the origin of cerebellar oligodendrocytes and interneurons, different rostro-caudal fragments were isolated from E12.5 cerebella of GFPU mice (Fig. 6A) and grafted to the telencephalon of P2 Swiss mice (Fig. 6B). Recipient animals were allowed to survive for 12 days (origin of oligodendrocytes, *N* of grafts = 5 per group) or 1 month (origin of interneurons, *N* of grafts = 7 per group). To determine the proportion of extracerebellar oligodendrocytes in cerebellar grafts, E12.5 primordia from wild type mice were implanted to the cerebellum of P2 βactin-GFP mice (5 animals per group). To study proliferation, embryos were fixed 2 h after intraperitoneal injection of BrdU (50 mg/kg in saline) to pregnant mice.

Ex-utero electroporation

biCS2 Ascl1/EGFP (gift from L. Turner, University of Michigan, Ann Arbor, MI) pEGFP-N1 (Clontech, Mountain view, CA, USA) expression vectors were electroporated into E14.5 CD-1 embryos ex-utero. The pregnant mouse was killed with CO_2 and the embryos were collected in PBS (with glucose and penicillin-streptomycin as above). The vectors were diluted at 1 μg/μl in PBS with 2.5 mg/ml fast green (Sigma, St Louis, MO, USA). To express *Ascl1*–GFP and pEGFP-N1 in ventricular progenitors, the plasmids were injected in the lumen of the diencephalic ventricle (Fig. 5C), so to prevent accidental puncture of the cerebellar tissue. As a control, the pEGFP-N1 was injected in the cerebellar parenchyma (Fig. 5M). Electroporation was performed with a BTX electroporator (Holliston, MA, USA) with the following parameters: 5 pulses, intensity = 70 V, pulse length = 50 ms, interpulse interval = 450 ms. At the end of the procedure, the brainstem and cerebellum were dissected and cultured for 6 days *in vitro* as described in Carletti et al. (2002). To evaluate the proliferation of electroporated cells, slices were kept *in vitro* for 24 h, exposed to BrdU for 30 min (3 mg/ml in the culture medium at 37 °C) and finally fixed 2 h later.

Immunohistochemistry and in situ hybridization

For immunohistochemical staining, embryos up to E16.5 were immersion-fixed in 4% paraformaldehyde (PFA) in 0.12 M phosphate buffer pH 7.2 (PB) for 2 h at 4 °C, and rinsed in PBS for 2 h. Embryos older than E16.5 and postnatal mice were perfused transcardially with the same fixative and postfixed overnight at 4 °C. The brains were cryoprotected with 30% sucrose in PBS until they sank and embedded in O.C.T. compound. The brains were cut in several series using a Leica cryostat (Wetzlar, Germany). Up to P7, 20 μm thick sections of the cerebellum were collected on Superfrost® Plus slides. Sections from older cerebella were 30 μm thick and processed free-floating. Primary antibodies for immunofluorescence were anti-Calbindin D28k (CaBP; mouse, monoclonal, 1:3000; Swant, Bellinzona, Switzerland); anti-Parvalbumin (PV; mouse, monoclonal, 1: 2000; Sigma), anti-Pax2 (rabbit polyclonal, 1: 200; Invitrogen), anti-RoRα (goat polyclonal, 1: 500; Santa Cruz Biotechnology, CA, USA), anti-Olig2 (rabbit polyclonal, 1:1000, Millipore USA), anti-NG2 (rabbit polyclonal, 1:500, Millipore), anti-GFP (chicken polyclonal, 1:2000, Aves Labs, Tigard, OR, USA), anti-BrdU (rat monoclonal, 1:500, Abcam,), anti-neuronal nuclei antigen (NeuN; mouse monoclonal, 1:1000; Millipore), anti glutamate astrocytic specific transporter (Glast, guinea pig, polyclonal, 1:1000, Millipore), anti-glial fibrillary acidic protein (GFAP, rabbit polyclonal, 1:1000; Dako-Cytomation, Glostrup, DK), Calretinin (mouse monoclonal, 1:100, Swant), anti-Sox9 (rabbit polyclonal, 1:2000, gift of R. Wegner, University of Erlangen, Erlangen, Germany). For BrdU immunohistochemistry, the slices were preincubated in HCl 2 N for 20 min at 37 °C, then washed in PBS and incubated in borate buffer (0.5 M, pH 8.5) for 10 min at room temperature. In all instances, the sections were incubated overnight at 4 °C in the different primary antibodies, diluted in PBS containing 0.25% Triton X-100 and 0.2% gelatin. Finally, the sections were washed in PBS and revealed for 1 h in secondary antibodies conjugated to Alexa fluor 488 (1:1000; Invitrogen) or cyan3 (Cy3, 1:1000, Jackson Immunolabs), and coverslipped using Mowiol (Calbiochem). Finally, in some cases, cell nuclei were stained with 4′-6-diamidino-2-phenylindole (DAPI, Fluka).

For *Ascl1* in-situ hybridization, after perfusion, the brains were collected in PFA, then washed in PBS and cut with a Leica (Wetzlar, Germany) vibratome, in 200 μm thick slices. We used an *Ascl1* antisense probe, following a previously established protocol (Wilkinson, 1992) with an ON incubation at 70 °C.

Data analysis

The histological preparations were examined by means of a Zeiss Axiophot light microscope (Karl Zeiss, Oberkochen, Germany) or a Leica DMRXA2 microscope. Micrographs were taken by means of a Leica DC 300F camera and Leica QFluoro software attached on the Leica microscope. The material was also examined with a Fluoview 300 confocal microscope (Olympus Optical, Hamburg, Germany) or with a Leica TCS SP2 confocal microscope. Digital images were processed with Adobe Photoshop 6.0 to adjust contrast and assemble the final plates.

Pax2 was used as a marker of cerebellar inhibitory interneuron progenitors (Maricich and Herrup, 1999; Weisheit et al., 2006) and Olig2 as a marker for OPC (Zhou and Anderson, 2002). In the cerebellum, Olig2 is also expressed in the deep cerebellar nuclei (DCN, Figs. 6H, H′, I–I″; Figs. 1A–C in Supplementary data). These neurons

were however readily distinguishable from the Olig2$^+$ OPCs, based on their clustering, position and morphology. In addition, the majority of them failed to incorporate BrdU pulsed at E15.5 (Fig. 1B, inset, in supplementary data). They could be easily excluded from all the quantitative estimations of Olig2$^+$ cells. Glast (Storck et al., 1992) and Sox9 (Stolt et al., 2003) were used to identify astrocyte progenitors.

Analysis of the E18.5 Ascl1$^{-/-}$ mouse

To estimate interneuron, oligodendrocyte or astrocyte progenitor numbers, we assessed the density of Pax2$^+$, Olig2$^+$ and Sox9$^+$ cells in E18.5 *Ascl1*$^{-/-}$ and wild-type embryos from the same litter. The number of the progenitors stained with these markers was counted on every fourth section over the whole cerebellum (20 μm parasagittal slices) and divided for the area of the section, calculated by NIH ImageJ software. The density of interneuron progenitors was estimated on 6 *Ascl1*$^{-/-}$ and 6 wild-type animals. OPCs were quantified on 5 *Ascl1*$^{-/-}$ and 5 wild-type animals. To rule out the possibility that the differences of cell densities were secondary to a variation of the cerebellar size in *Ascl1*$^{-/-}$ mice, we made a 3D reconstruction of 3 knock-out and 3 wild type cerebella by means of the Amira software (Visage Imaging GmbH, Berlin, Germany). These cerebella were cut in 20 μm-thick transversal slices, stained with DAPI and anti-Calbindin antibodies to visualize the boundaries of the cerebellum.

Analysis of the grafted minicerebella

To quantify the number of interneurons in the *Ascl1*$^{-/-}$ and GFP$^+$ cerebellar transplants, we counted the number of PV$^+$ interneurons. In addition, the number of Calbindin$^+$ Purkinje cells was determined as an index of the graft size. The results were also expressed as the ratio Int/PC. Twelve grafts from *Ascl1*$^{-/-}$ and 13 from their matched controls were analysed (Fig. 4D). In addition, 7 grafts of rostral cerebellum and 7 from the caudal part were examined (Fig. 6C). The density of OPCs was estimated on single E12.5 grafts implanted to P4 host cerebella; the area of the relevant slice was measured with NIH software ImageJ. To determine whether OPC originating from extracerebellar territories populate the cerebellar anlage, we implanted solid grafts of E12.5 cerebella to the cerebella of P2 βactin-GFP mice. In these grafts we estimated the frequency of host-derived OPCs by counting Olig2$^+$GFP$^+$ cells on single confocal sections (*N* of grafts = 4 in each case; a minimum of 100 cells were counted in each graft), and divided their number for the surface area of the graft (estimated by ImageJ as above). In addition, to estimate the relative frequency of endogenous and immigrating OPCs in the cerebellar transplants, we calculated the ratio of Olig2$^+$GFP$^+$ cells on the total of Olig2$^+$ cells in the graft area.

Analysis of Ascl1 and GFP electroporation

The percentage of the electroporated cells positive for the different markers (Pax2, Olig2, Glast, and BrdU) was estimated as the frequency of double labelled cells over the whole population of GFP$^+$ elements. The density of electroporated cells was calculated by dividing the number of GFP$^+$ cells for the size of the microscopic field at 20× magnification (area of the field = 0.48 mm^2), in single confocal sections. In all instances, the statistical significance of was calculated by means of the Student's *T* test. All the data are given as mean ± s.d.

Results

Ascl1 is expressed by the progenitors of interneurons and oligodendrocytes

To clarify the role of *Ascl1* in the development of OPCs and GABAergic interneurons in the cerebellum, we first studied its expression pattern during embryonic and postnatal development, when these cells are generated. Consistent with previous reports (Zordan et al., 2008), *Ascl1* mRNA is already detectable in the cerebellar primordium at E12.5 (not shown). By E16.5 (Fig. 1A) it is expressed in the VZ, but not in the rhombic lip, with sparse *Ascl1*$^+$ cells in the subventricular zone (arrows in Fig. 1A). By E18.5, the expression in the VZ fades out and numerous *Ascl1*$^+$ cells are scattered throughout the prospective WM (Fig. 1B). This distribution persists after birth, when numerous labelled cells are also present in the nascent cortical layers (Figs. 1C, D). Thus, the distribution of *Ascl1*$^+$ during the examined period is suggestive of VZ progenitors that progressively delaminate into the prospective WM and eventually colonize the cortex.

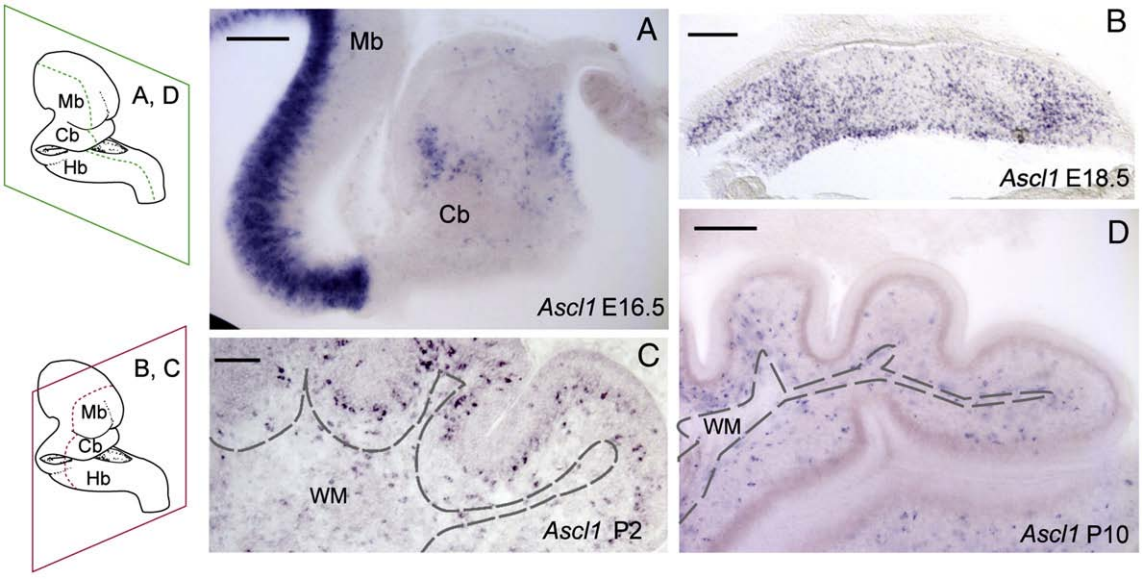

Fig. 1. Time course of *Ascl1* expression in the developing cerebellum. Transverse (A, B) and sagittal (C, D) sections of E16.5 (A), E18.5 (B) P2 (C) and P10 (D) cerebella treated for the detection of Ascl1 transcripts by in situ hybridization. The orientation of the sections in each row is schematized on the left. At E15.5 (A), *Ascl1* is mainly expressed in the ventricular zone (VZ), some *Ascl1*$^+$ cells start to colonize the cerebellar parenchyma (arrows). By E18.5 (B), Ascl1-expressing progenitors lie in the white matter. In the P2 (C) and P10 (D) cerebellum, Ascl1-expressing lay in the white matter (dotted line) and in the nascent cortical layers. Mb: midbrain, Cb: cerebellum, Hb: hindbrain). Calibration bar: 100 μm in A, B, D, 50 μm in C.

To define the fate of *Ascl1*-expressing cells, we took advantage of *Ascl1::GFP* transgenic mice, in which the reporter persists longer than Ascl1. The *Ascl1::GFP* transgenic line has been extensively studied and found to be a reliable tracer for short term lineage studies in embryos and in adult neurogenesis. Purkinje cells (Fig. 2A) were GFP$^+$ and exhibited regional variations in the intensity of expression of the

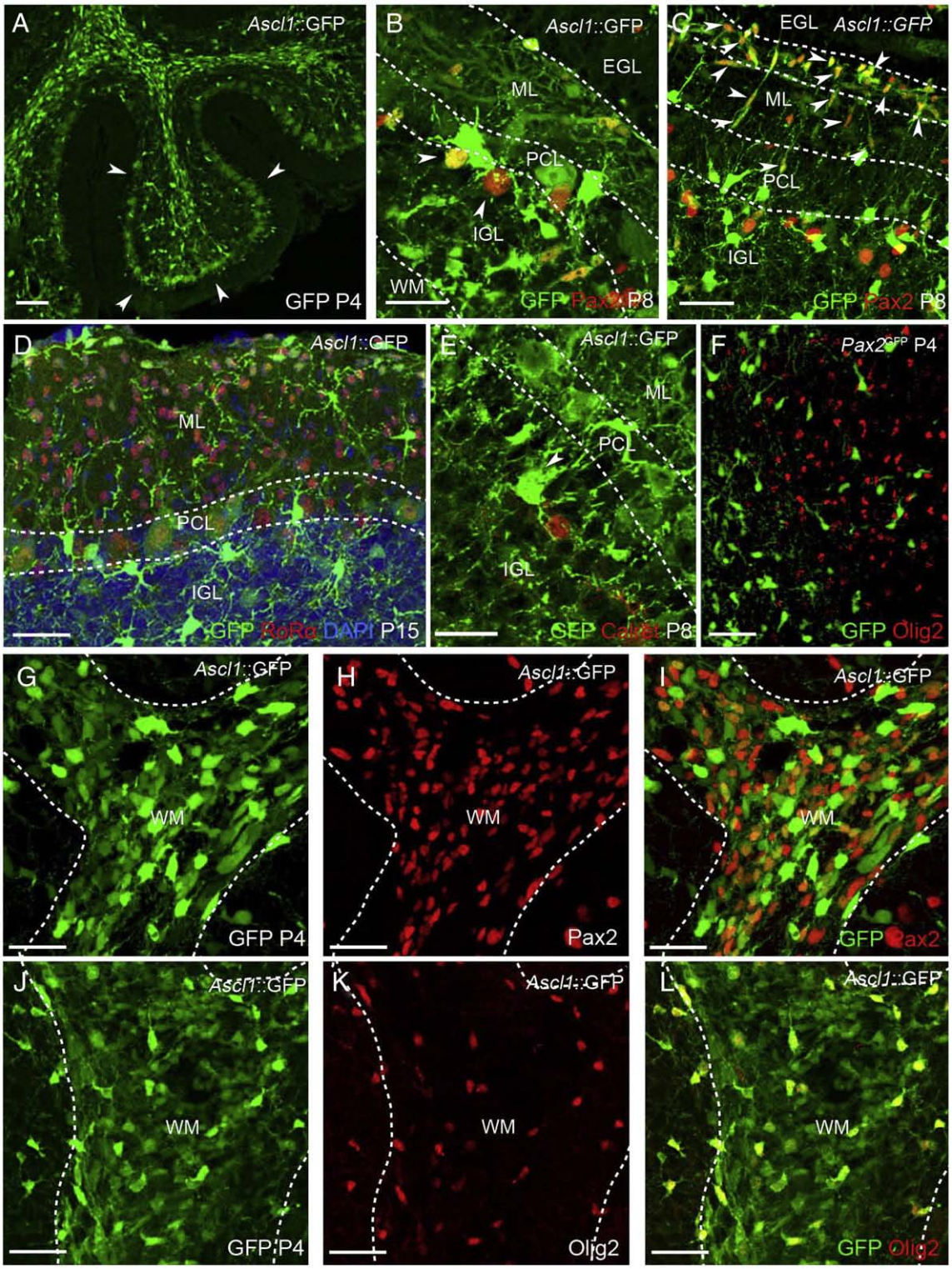

Fig. 2. Characterization of the *Ascl1* lineage in *Ascl1::GFP* (A–E, G–L) and *Pax2^{GFP}* (F) mice. Sagittal sections. In the *Ascl1::GFP* mouse, all GABAergic neurons are labelled by GFP (A–D, G–L). (A) Low magnification of the P4 cerebellum. Purkinje cells (arrows) and white matter progenitors are labelled by GFP. (B) Golgi cells (arrows) are faintly labelled by GFP in the P8 cortex of the *Ascl1::GFP* mouse. C shows Pax2$^+$ interneuron progenitors migrating in the cortical layers and differentiating in the upper ML beneath the EGL. (D, E) In contrast to GABAergic neurons, glutamatergic interneurons are GFP negative: granule cells (blue labelled by DAPI in D) and Calretinin$^+$ unipolar brush cells (red, arrow in E) are not labelled by the GFP (green). (F) Olig2 (red) and GFP (green) do not colocalize in the cerebellar white matter of a P4 *Pax2^{GFP}* transgenic mouse, indicating that the interneuron and oligodendrocyte lineages are segregated. (G–L) In the cerebellar white matter at P4 the *Ascl1::GFP* transgene is co-expressed either with Pax2 (red G, I) or with Olig2$^+$ (red in J, L). IGL: internal granular layer, PCL: Purkinje cell layer, ML: molecular layer, EGL: external granular layer, WM: white matter. Calibration bars: 20 μm in A, B, D, F–L, 10 μm in C, E.

Table 1
Density of progenitor and proliferating cells in the E18.5 *Ascl1*$^{-/-}$ and WT mouse

	Ascl1$^{-/-}$	WT	*P*
Pax2 cells/mm^2	212.06 ± 101.49	836.97 ± 276.56	$P=0.003$
Olig2 cells/mm^2	183.59 ± 56.91	515.88 ± 136.35	$P=0.001$
Sox9 cells/mm^2	1935.55 ± 96.48	1631.09 ± 150.36	$P=0.042$
PH3 cells/mm^2	46.56 ± 6.91	70.90 ± 17.06	$P=0.038$

Ascl1::GFP transgene. At different ages from P4 to P14, we consistently found Pax2 and Olig2 expression in GFP$^+$ cells (Figs. 2B, C, G–L). This suggests that both oligodendrocyte progenitors and GABAergic neuron progenitors express Ascl1. On the contrary, deep nuclei neurons and glutamatergic interneurons, such as granule cells (blue labelled by DAPI in Fig. 2D) or unipolar brush cells (Fig. 2E), as well as astrocytes and Bergmann glia never displayed GFP fluorescence. Pax2$^+$ and Olig2$^+$ GFP$^+$ cells were found in the prospective WM and in the cortical layers (Figs. 2B, C, G–L). The results of in situ hybridization experiments shown in figure A, in keeping with previously published studies, indicate that Ascl1 is expressed starting early in GABA progenitor development. In addition, the localization of GFP$^+$ cells in the cortex (Figs. 2B, D) is consistent with the spreading of maturing oligodendrocytes and interneurons. Thus, this expression pattern indicates that both these lineages express *Ascl1* during their development. However, the absence of cells coexpressing Pax2 and Olig2 (by double-immunolabelling or Olig2 staining in Pax2-GFP mice, Fig. 2F) indicates that, at least from the stage when these markers are upregulated, *Ascl1*$^+$ cells comprise two distinct populations.

Ascl1$^{-/-}$ *loss of function alters the development of interneurons, oligodendrocytes and astrocytes*

In order to assess the role of Ascl1 in the development of cerebellar inhibitory interneurons, oligodendrocytes, and astrocytes, we analysed the phenotype of the *Ascl1*$^{-/-}$ mutant mouse. Since *Ascl1* mutation is lethal soon after birth, we first analysed the E18.5 embryo (summarized in Table 1). We used Pax2 as a marker of interneuron progenitors (Maricich and Herrup, 1999; Weisheit et al., 2006) and Olig2 as a marker for OPCs (Zhou and Anderson, 2002). Sox9 has been recognized as a marker of several neural crest derivatives (Spokony et al., 2002, Cheung and Briscoe, 2003) as well as a marker of astrocyte precursors (Stolt et al., 2003). The number of proliferating cells was evaluated by counting the phospho-histone H3 labelled mitotic cells. In the mutant animals, Pax2$^+$ and Olig2$^+$ cells were dramatically reduced (Pax2$^+$ cells/mm^2: 212.06 ± 101.49; in *Ascl1*$^{-/-}$ mice, 836.97 ± 276.56 in WT controls, $N=5$ for both groups, tot cells counted: 27,277; $P=0.003$, (Figs. 3A, A′, B); Olig2$^+$ cells/mm^2 in *Ascl1*$^{-/-}$ mice = 183.59 ± 56.91, in WT controls = 515.88 ± 136.35, $N=5$ for both groups, tot cells counted = 25,831; $P=0.001$, Figs. 3C, C′, D), whereas Sox9$^+$ progenitors were moderately increased (Sox9$^+$ cells/mm^2: 1935.55 ± 96.48; in *Ascl1*$^{-/-}$ mice, 1631.09 ± 150.36 in WT controls, $N=3$ for both groups, tot cells counted: 30148; $P=0.042$, Figs. 3E, E′, F). PH3 immunolabelling revealed a moderate but significant reduction of the amount of dividing cells in the *Ascl1*$^{-/-}$ cerebellum (PH3$^+$ cells/mm^2 in the *Ascl1*$^{-/-}$: 46.56 ± 6.91; PH3$^+$ cells/mm^2 in the WT: 70.91 ± 17.06, $N=4$ in both groups, tot cells counted = 2898; $P=0.038$, Figs. 3G, G′, H). Olig2 based OPC counts had to avoid a deep nuclear subdivision containing Olig2$^+$ neurons (Supplementary Fig. 1). We confirmed that the reduction in Olig2$^+$ cells in E18.5 *Ascl1*$^{-/-}$ faithfully reflected a decrease in the number of cerebellar OPC by using two additional OPC markers, PDGFRa (Figs. 3I, I′) and NG2 (Figs. 3J, J′). As the mutant vermis often appeared slightly smaller compared to wild type, to ascertain that the differences observed in the above estimates were not a consequence of an altered size of the mutant cerebella, we reconstructed the volume of three WT and three *Ascl1*$^{-/-}$ cerebella. The slight volumetric decrease observed in mutant animals was not statistically significant (mean volume: *Ascl1*$^{-/-}$ = 1.49 mm^3 ± 0.01; WT = 1.75 mm3 ± 0.16, $P=0.078$ Figs. 4A–B′), and cannot account for the different cell densities observed.

To further define the effect of *Ascl1* loss of function at more advanced developmental stages, we took advantage of the known property of embryonic cerebellar tissue to develop minicerebella after heterotopic transplantation. Thus, we implanted solid pieces of E15.5 cerebella from wild-type and mutant mice into the telencephalon of newborn recipients. One month later, we estimated the numbers of Purkinje cells and of PV immunopositive interneurons (Celio, 1990) of the molecular layer. The average number of Purkinje cells was 823.5 (±452.13, Fig. 4C) in *Ascl1*$^{-/-}$ grafts and 646.8 (±434.92 Fig. 4C′) in their wild-type counterparts. The values were not statistically different ($P=0.31$). In contrast, interneurons were significantly reduced from 931 (±676.34, Fig. 4C) in wild-type to 361.3 (±142.76, Fig. 4C′) in *Ascl1*$^{-/-}$ grafts ($P=0.02$), and the ratio ML int/PC changed from 1.4 ± 0.35 in control to 0.51 ± 0.23 in *Ascl1*$^{-/-}$ grafts (Figs. 4C, C′, D; $P<0.001$). Purkinje cells are subdivided into subtypes characterized by their distinct levels of expression of various markers including Calbindin and EphA4. In Purkinje cells, subtype identity is correlated to birthday (Hashimoto and Mikoshiba, 2004; Wassef et al., 1985). We wondered if *Ascl1* could be involved in Purkinje cell differentiation or subtype choice. The patterns of expression of Rorα (Supplementary Figs. 2A–D) Calbindin (Supplementary Figs. 2E, F) or EphA4 (Supplementary Fig. 2G) were not modified in E18.5 *Ascl1*$^{-/-}$ embryos compared to wild type. Therefore, the loss of *Ascl1* function in mutant mice has no major effect on Purkinje cell development, but severely impairs the development of GABAergic interneurons, and this defect is not compensated even at long survival times.

Prospective analysis of VZ progenitors and effect of Ascl1 overexpression

The observations reported in the previous sections, in line with previous data in the developing olfactory bulb (Parras et al., 2004), show that, in the cerebellum, oligodendrocyte and interneuron progenitors express *Ascl1*, and that the lack of this gene results in a reduction of both cell types. In order to start investigating whether the two cell types are lineally related in the cerebellum, we studied whether they originate from a common region in the VZ or from distinct territories. For this purpose, we labelled the VZ by electroporation with a GFP-expressing vector, injected into the lumen of the fourth ventricle at E14.5 (Fig. 5A), when the first interstitial progenitors are labelled with BrdU (Leto et al., 2006 and personal observation). After electroporation, the cerebella were dissected and cultured for 6 days before histological examination (Fig. 5C). Out of a total of 1342 GFP$^+$ cells from 5 electroporated cerebella, 20.7% (±14.1, Figs. 5B, C, F) were Pax2$^+$ interneuron progenitors. Quite surprisingly, only 2.4% (±1.5, tot cell number = 794 Figs. 5B, G) were Olig2$^+$ cells, while a consistent fraction of GFP$^+$ cells were colabelled with astrocytic markers Glast (9.5% ± 0.3 tot cell number = 1930, $N=4$ Figs. 5B, E) as well as GFAP (not shown) and S100b (Fig. 5I).

To validate the technique and show that oligodendrocytes can develop in our culture paradigm, we repeated the electroporation after injection of the GFP plasmid into the parenchyma instead of the ventricle (Fig. 5M). Intraparenchymal electroporations labelled a higher number of Olig2$^+$ cells (13.5% ± 6.6; Figs. 5N–P) the proportion

Fig. 3. *Ascl1* loss of function affects several cerebellar cell types. Representative sagittal sections of wild type (A′, C′, E′, G′, I′, J′) and *Ascl1*$^{-/-}$ mutant (A, C, E, G, I, J) cerebella at E18.5. Comparison of the density of interneurons (A, A′, B; stained for Pax2 in green), oligodendrocytes (C, C′, D, stained for Olig2 in green, I, I′ stained for PDGFRα in purple, J, J′ stained for NG2 in purple), astrocytes (E, E′, F, stained for Sox9 in green) and mitotic cells (G, G′ H stained for phosphohistone H3, PH3 in red). The surface densities (cells/mm^2) of the different cell types are compared between wild type and mutants in Charts B (Pax2$^+$), D (Olig2$^+$), F (Sox9$^+$) and H (PH3). Calibration bar: 200 μm in A–H, 100 μm in I–J′.

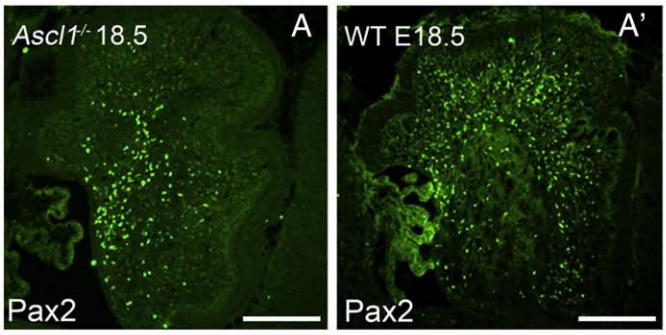

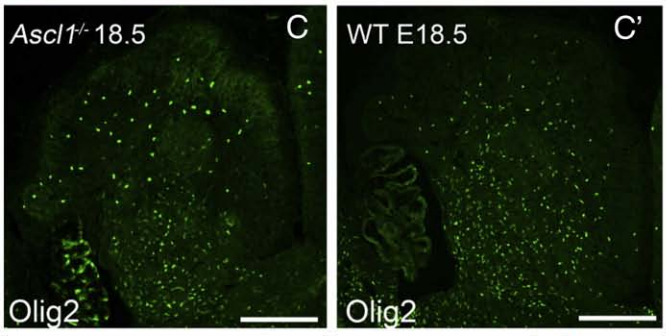

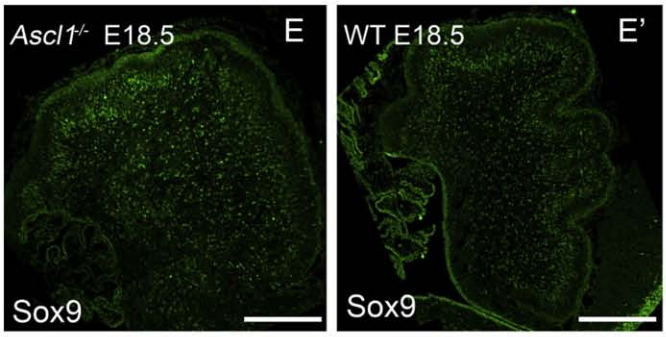

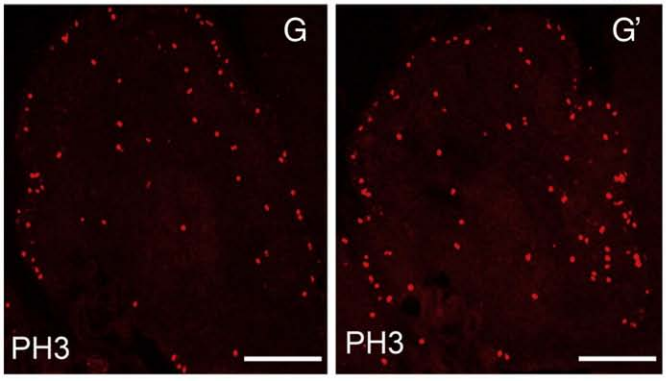

B Density of interneuron progenitors in the *Ascl1*$^{-/-}$ and WT E18.5 cerebellum

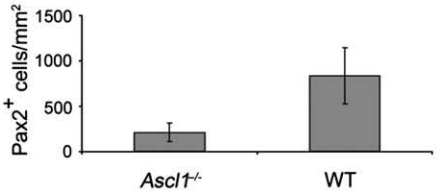

D Densty of OPCs in the *Ascl1*$^{-/-}$ and WT E18.5 cerebellum

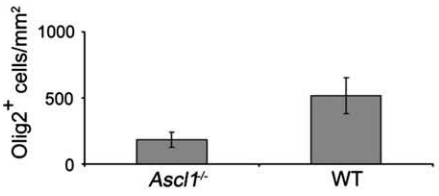

F Density of astrocyte progenitors in the *Ascl1*$^{-/-}$ and WT E18.5 cerebellum

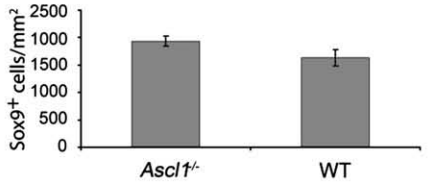

H Density of PH3^{+} cells in the *Ascl1*$^{-/-}$ and WT E18.5 cerebellum

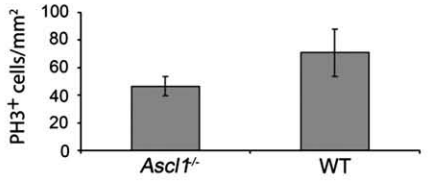

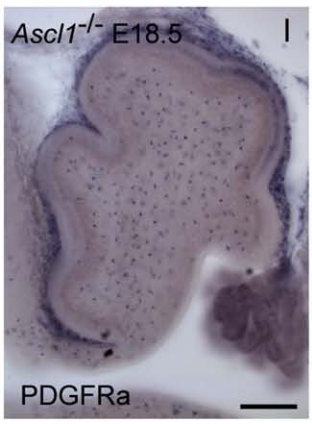

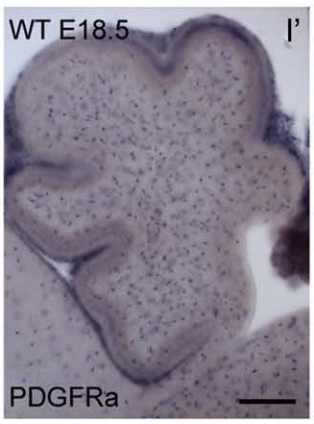

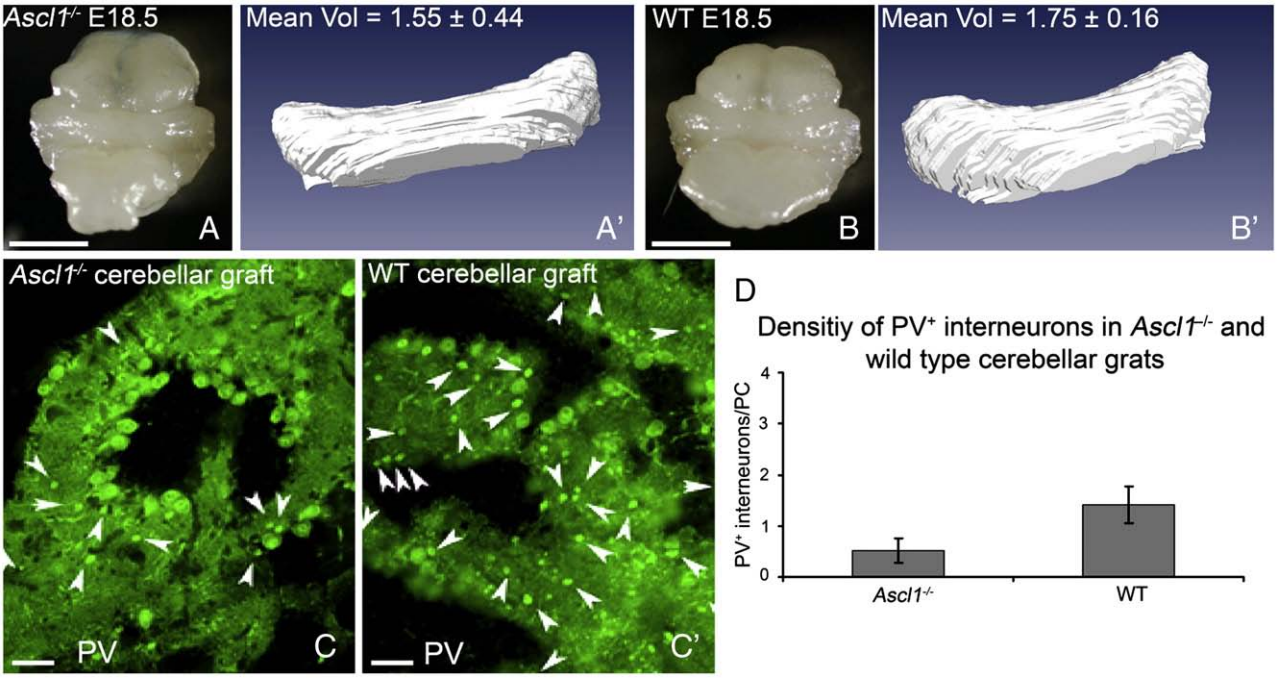

Fig. 4. Comparison of the volume of the *Ascl1*$^{-/-}$ and WT cerebellum at E18.5 and grafts of *Ascl1*$^{-/-}$ cerebella. External aspect (A, B) and 3D reconstruction (A′, B′) of the cerebella of E18.5 *Ascl1*$^{-/-}$ (A, A′) and WT (B, B′) littermates. (C–C′). Transplants of E14.5 *Ascl1*$^{-/-}$ (C) and WT (C′) cerebellar fragments grown in vivo and stained with Parvalbumin for the detection of mature molecular layer GABAergic interneurons (arrowheads). The proportion of GABAergic interneurons/Purkinje cells is illustrated on Chart D. Calibration bar: 500 μm in A, B; 20 μm in C.

of GFP$^+$ elements expressing Olig2 was statistically different from that observed after intraventricular plasmid injection (tot cells counted = 1645, $N = 4$ in both cases, $P = 0.029$). These experiments show that at E14.5, progenitors in the VZ give origin to interneurons and astrocytes, but rare oligodendrocytes. By this time, however, precursors of the latter cell type are present within the cerebellar parenchyma.

Since the loss-of-function experiments show that *Ascl1* is required for the generation of both oligodendrocytes and interneurons and previous gain-of-function experiments suggested that *Ascl1* can promote either oligodendrocyte or interneuron fate depending on the cellular context (Mizuguchi et al., 2006; Jessberger et al., 2008), we decided to check whether *Ascl1* overexpression could bias the fate of cerebellar VZ progenitors towards the oligodendroglial and/or interneuronal lineage. Therefore, we induced *Ascl1* overexpression by electroporation of an *Ascl1*–GFP construct, injected into the ventricular lumen to selectively target superficial cells (Fig. 5D). Six days later, the great majority of GFP$^+$ cells expressed Pax2 (81.50% ± 6.34, $N = 5$, tot cell number = 2181, against 20.68% ± 14.13 after GFP electroporation, $P < 0.001$, Figs. 5B, H–H″), whereas Olig2$^+$ OPCs were even fewer than in GFP-electroporated controls (1.31% ± 1.42, tot cell number = 858, $N = 4$), and Glast$^+$GFP$^+$ cells were completely absent (Fig. 5B). As shown by BrdU-incorporation experiments (Fig. 5K), Pax2$^+$ cells likely represent postmitotic interneuron progenitors (Weisheit et al., 2006). Therefore, in the developing VZ, Ascl1 forced expression induces the differentiation of progenitors into interneurons and not oligodendrocytes. Together with this, Ascl1 overexpression seems to repress astrocytic differentiation.

To determine whether Ascl1 directs the fate choice of uncommitted VZ progenitors towards the interneuron lineage or favours the survival of Pax2-expressing cells, we quantified the density of electroporated cells (Fig. 5J). If Ascl1 acts by selecting progenitors restricted to a GABAergic fate, one would expect a lower amount of GFP$^+$ cells in Ascl1–GFP-electroporated explants than in GFP-electroporated ones and a comparable number of GABAergic interneurons. On the other hand, if *Ascl1* biases uncomitted progenitors to the interneuron phenotype, the density of Pax2$^+$/GFP$^+$ cells should increase in the Ascl1-electroporated explants. Indeed, we found similar numbers of GFP-expressing cells in explants electroporated with GFP (159.31 ± 58.73 GFP$^+$ cells/mm^2) and with *Ascl1*–GFP (196.44 ± 72.36 GFP$^+$ cells/mm^2, $N = 5$, in both cases, $P = 0.391$, Fig. 5J). On the other hand, Pax2$^+$GFP$^+$ cells were substantially increased after Ascl1–GFP electroporation (31.86 ± 18.05 GFP$^+$ cells/mm^2 after GFP electroporation, 164.46 ± 31.45 GFP$^+$ cells/mm^2 after Ascl1 electroporation, $N = 5$, $P < 0.001$, Fig. 5J).

To further rule out a selective effect of *Ascl1*, we stained the explants with anti-caspase 3 antibody, 2 days after electroporation. We observed no significant co-localization of GFP and caspase 3 staining in GFP-electroporated, or in *Ascl1*-electroporated explants (data not shown).

To exclude the possibility that Ascl1 overexpression modifies the proliferation dynamics of transfected cells, we made a pulse of BrdU 1 day after electroporation. With both vectors, we found similar numbers of electroporated cells that incorporated BrdU (10.31 ± 4.67% BrdU$^+$GFP$^+$/GFP$^+$ cells after GFP electroporation, 12.91 ± 7.84% BrdU$^+$GFP$^+$/GFP$^+$ cells after *Ascl1* electroporation, $N = 4$. $P = 0.55$ Figs. 5K, L). Together, these results indicate that *Ascl1* overexpression biases the phenotypic choice of VZ progenitors towards a GABAergic interneuron identity and suppresses the astrocytic fate.

Separate origins for cerebellar interneurons and oligodendrocytes

Since GFP electroporations of the cerebellar VZ at E14.5 failed to label oligodendrocytes while GABAergic interneurons were transfected, we asked whether these lineages derived from distinct germinal sites or shared a common origin at earlier ontogenetic stages. We compared the cellular composition of solid grafts dissected from the rostro-medial or caudo-lateral portions of the E12.5 cerebellar anlage (Figs. 6A–C). As for *Ascl1*$^{-/-}$ grafts, fragments from donor βactin-GFP mouse were implanted in the telencephalon of P2 wild-type mice and examined 30 days later. To compare the density of interneurons in the different transplants, the number of PV$^+$ molecular layer interneurons was normalized on that of Purkinje cells present in the same section. As

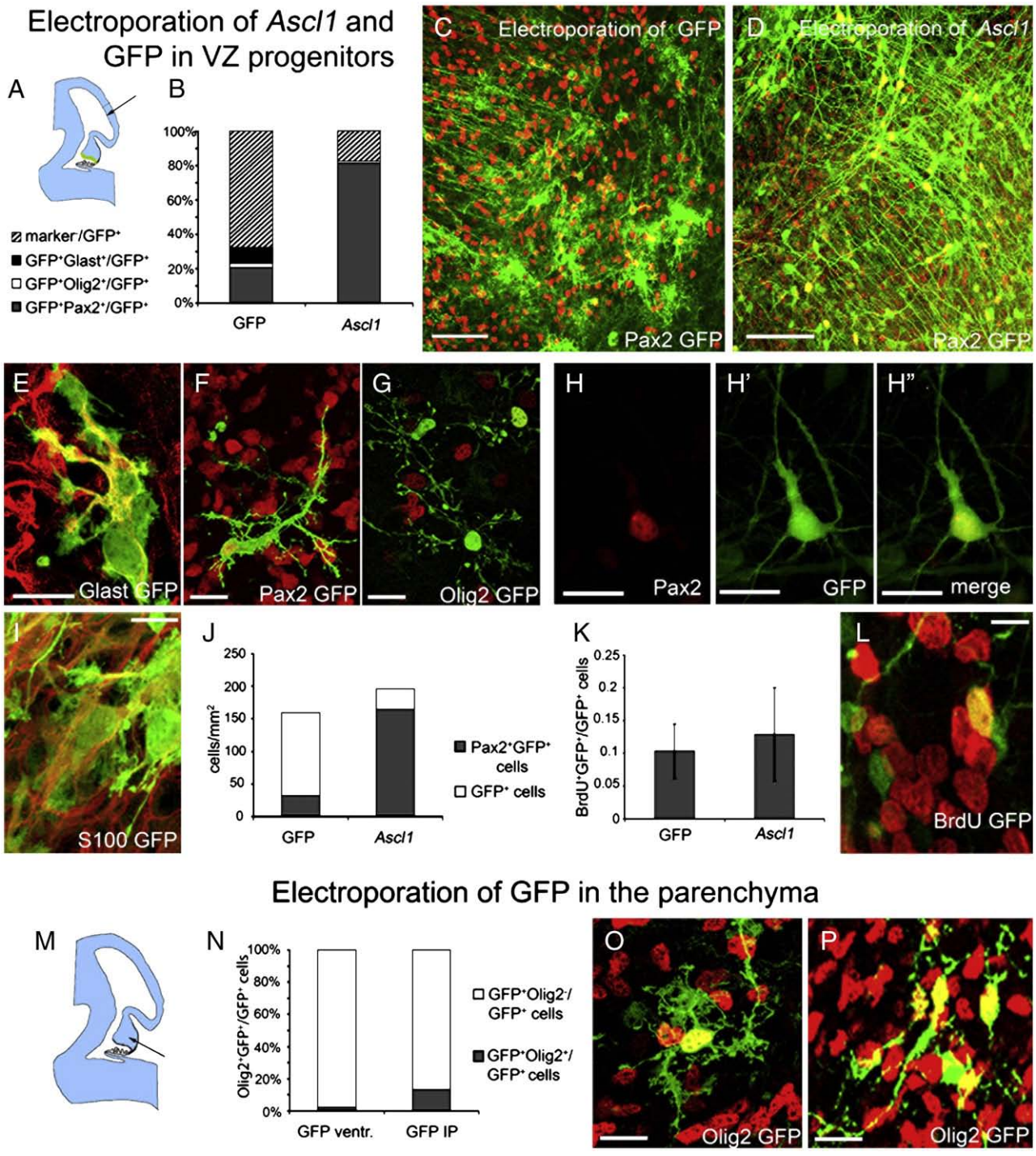

Fig. 5. GFP and *Ascl1* expression in the cerebellar neuroepithelium at E14.5. (A–L) pEGFP-N1 (GFP control) and *Ascl1*–GFP constructs were injected in the fourth ventricle of E14.5 mouse embryo as schematized in (A) and electroporated in the cerebellar neuroepithelium (green). The cerebellar slices were fixed after 6 days in culture. (C, D) Low magnification of slices immunostained for GFP (green) and Pax2 (red). Whereas after GFP control electroporation there is a great variability of cell morphologies (A), *Ascl1*–GFP electroporated slices virtually show only one morphological type of GFP-labelled cells (D). The percentages of cells positive for the different markers tested after are illustrated in Chart B for control GFP and *Ascl1*–GFP electroporations. The main GFP^+ cell types identified in GFP-electroporated embryos were interneurons and astrocytes, the majority expressed none of the markers tested. In contrast, most *Ascl1*–GFP electroporated cells were $Pax2^+$ interneuron progenitors. Panels E–G and I detail the cell types identified in GFP-electroporated slices: Glast (E) and S100b (I) immunoreactivities identify astrocyte precursors, Pax2 marks GABAergic interneurons (F), Olig2 labels oligodendrocytes (G). After *Ascl1* electroporation, virtually all GFP-expressing cells had an interneuron morphology, and about 80% cells expressed Pax2 (H). (J) densities of GFP^+ and of $GFP^+/Pax2^+$ cells after electroporation of control GFP or *Ascl1*–GFP. I, L) analysis of proliferation after electroporation of control GFP or *Ascl1*–GFP. The percentage of $BrdU^+$ cells is not significantly altered after electroporation of *Ascl1*–GFP (K). (L) Illustrates a GFP^+ cell that incorporated BrdU after pEGFP-N1 electroporation. (M–P) GFP electroporation in the cerebellar parenchyma the site of plasmid injection is schematized in (M). (N) Percentage of $Olig2^+/GFP^+$ after electroporation of GFP in the ventricular zone and in the parenchyma. (O) $Olig2^+$ (red) OPCs in electroporated slices. (P) Shows a Olig2-expressing DCN. Calibration bar: 20 μm in A, D, 10 μm in E–H, O, P, 5 μm in J, L.

shown in Chart C, rostro-medial grafts were highly enriched with interneurons (PV^+ interneurons/PV^+CaBP^+ cells = 2.22 ± 1.30, $N = 7$), whereas their caudo-lateral counterparts appeared severely depleted (PV^+ interneurons/PV^+CaBP^+ cells = 0.35 ± 0.46, Fig. 6C), showing that the rostro-medial part of the cerebellar anlage provides a major source of GABAergic interneurons.

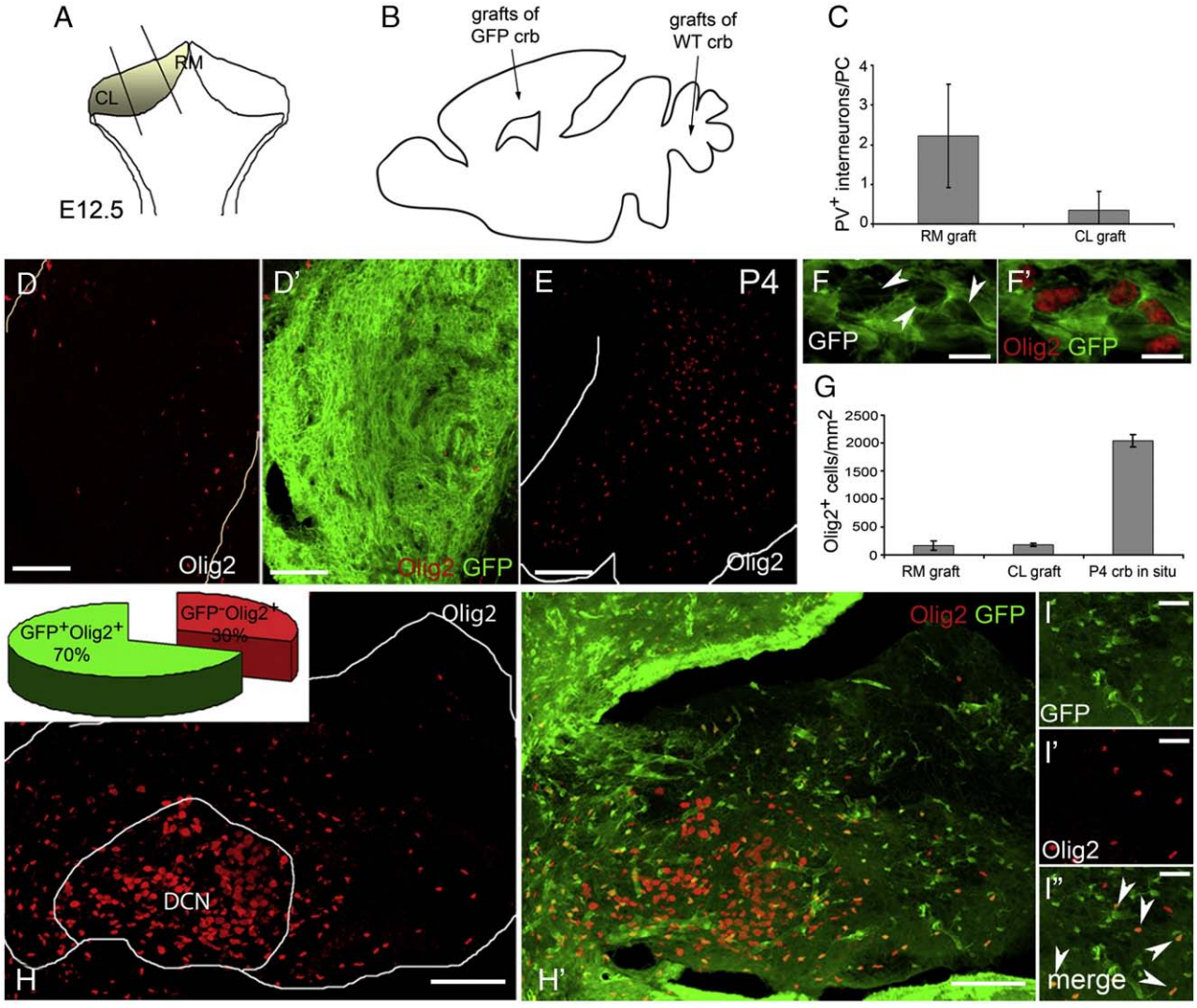

Fig. 6. Grafts of partitioned embryonic cerebella. (A–H) E12.5 grafts of partitioned cerebella from EGFP transgenic mice to the newborn mouse forebrain. (A) Schematic representation of the sites of origin of the transplanted fragments on a posterior view of the E12.5 cerebellum (RM = rostro-medial cerebellum, CL = caudo-lateral cerebellum). (B) Schematic representation of the site of implantation in the postnatal recipient mouse. Cerebellar fragments from GFP^+ mice were grafted to the telencephalon of P2 WT mice, while cerebella from WT mice were grafted to the cerebellum of $GGFP^+$ P2 mice. (C) Comparison of the ratio of PV^+ interneurons/PC in cerebellar transplants originating from the rostro-medial or caudo-lateral domains of E12.5 GFP^+ mice. The ratio is higher in rostral than in caudal grafts (C). (D) A GFP^+ minicerebellum fixed 12 days after transplantation contains few $Olig2^+$ OPC. (E) Sagittal section of an age-matched cerebellum illustrating the density of $Olig2^+$ OPCs by P4. (F) Higher magnification illustrating that the majority of oligodendrocytes do not express GFP in the grafts (F, arrowheads). (G) Density of $Olig2^+$ cells in E12.5 cerebellar grafts and in the age-matched cerebellum. (H, H′) Graft of a WT E12.5 cerebellum to a GFP^+ P2 cerebellum sacrificed 12 days after grafting. (H) shows $Olig2^+$ DCN and oligodendrocytes. (H′) illustrates the GFP labelled cells and processes originating from the GFP^+ host. Higher magnification (I) shows that the majority of $Olig2^+$ cells are GFP^+ (I″, arrowheads). The inset in (H) shows the percentage of $Olig2^+GFP^-$ and $Olig2^+GFP^+$ cells on the total amount of $Olig2^+$ cells in the grafts. Calibration bar: 50 μm in D, 5 μm in F, J, 20 μm in H.

The same approach was used to assess the distribution of the oligodendrocyte progenitors, made by quantifying $Olig2^+$ cells 12 days post transplantation. Both rostro-medial and caudo-lateral grafts contained fairly similar amounts of $Olig2^+$ cells (241.84 ± 149.54 cells/mm^2 in rostral grafts, 324.69 ± 57.24 cells/mm^2 in caudal grafts, $N = 3$ in both cases, $P = 0.25$, Figs. 6D, G), suggesting that this lineage does not derive from a restricted site within the anlage. However, the amount of these cells, was about 10-fold lower than that present in non manipulated aged-matched cerebella in situ (2041.14 ± 114.29 cells/mm^2, $N = 3$, P with the mean value of rostro-medial and caudo-lateral grafts, $283.01 \pm 111.25 < 0.001$, Figs. 6E–G). In addition, many $Olig2^+$ cells were not GFP^+ (Fig. 6F), indicating that a fraction of the oligodendrocytes that populate the transplant were actually derived from the host. Together with the results of electroporation experiments showing that the $Olig2^+$ cells in the E14.5 cerebellum cannot be labelled by vectors targeted to the VZ, these observations raised the possibility that the donor cerebellar tissue has limited endogenous oligodendrogenic capabilities. This implies that at least part of the cerebellar oligodendrocytes immigrate from an external germinal site and populate the cerebellum secondarily.

To test this hypothesis, we first studied the distribution pattern of $Olig2^+$ cells in the developing cerebellum. Olig2 starts to be expressed at E11.5 in the ventricular region and in the nuclear transitory zone (data not shown), its expression is maintained at E13.5 in both regions (Fig. 1A in Supplementary data). Olig2 expression in the ventricular layer is reduced from E15.5 on (Fig. 1B in Supplementary data) but maintained in the cerebellar parenchyma where it is detectable in clustered cells in the DCN region and in scattered presumptive OPC. The scattered population of Olig2-expressing cells, first appears at E15.5 (Fig. 1B in Supplementary data) and become numerous at E18.5 (Fig. 1C in supplementary data). Several features distinguish the $Olig2^+$ DCN neurons from OPC: their characteristic clustering, their size (not shown), their absence of labeling after a BrdU pulse at E15.5 (inset in Fig. 1B Supplementary data), and their expression of the neuronal

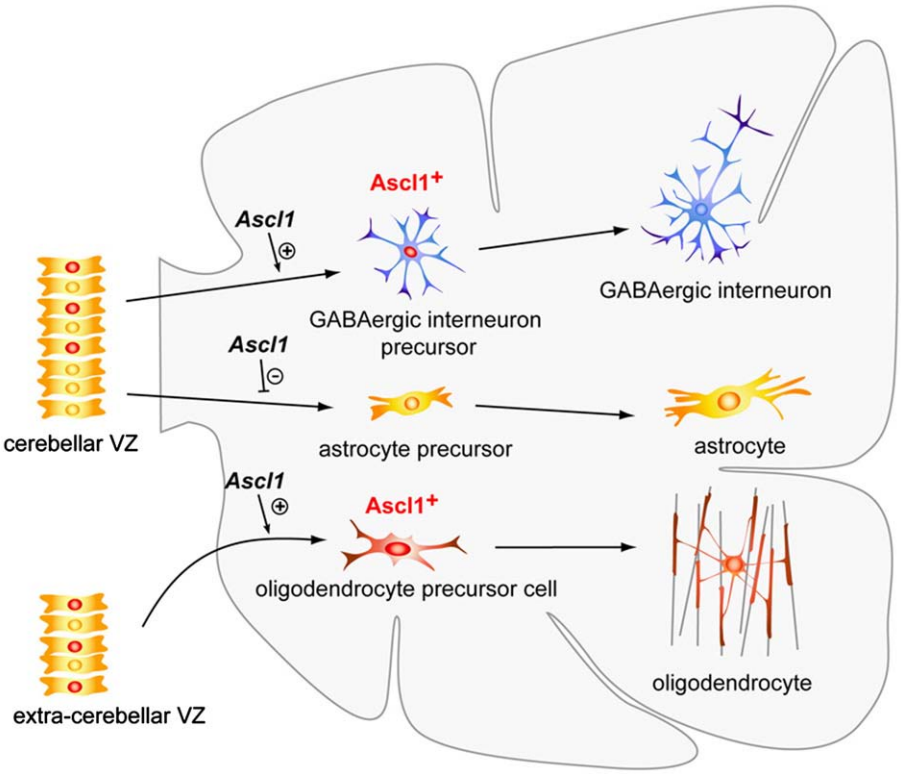

Fig. 7. Model of the specification of inhibitory interneurons and glia in the cerebellum. The schema represents an outline of the postnatal cerebellum. Oligodendrocyte progenitors which colonise the cerebellum early in development are generated from an extracerebellar neuroepithelial site, whereas inhibitory interneurons and astrocytes originate from the cerebellar ventricular zone. Ascl1 expression in ventricular zone progenitors drives interneuron differentiation and suppresses astrocyte generation.

marquer NeuN (Figs. 1D–F in Supplementary data). A few Olig2$^+$ cells also appear at the tip of the RL at E15.5 (Fig. 1G in Supplementary data). To quantitatively estimate the contribution of foreign OPCs to the contingent of cerebellar oligodendrocytes, we implanted E12.5 solid cerebellar wild type grafts into the cerebella of P2 βactin-GFP mice (Figs. 6H, H′, I–I″). These transplants contained 492.17 ± 171.74 Olig2$^+$ cells/mm^2 ($N = 4$, tot cells counted = 582), of which 69% (339 ± 102, tot cells counted = 1302, inset in H) were also labelled by GFP. This result supports the conclusion that the E12.5 cerebellar anlage contains a minor fraction of OPCs, and that the majority of cerebellar oligodendrocytes actually derive from extracerebellar sites.

Discussion

To elucidate the molecular determinants that regulate the generation of different cerebellar phenotypes, we investigated the role of *Ascl1*. We show that this gene is expressed in maturing oligodendrocytes and GABAergic interneurons and is required to produce appropriate amounts of both cell types. These two lineages, however, are not related: GABAergic interneurons originate from the rostro-medial region of the cerebellar primordium (see also Maricich and Herrup, 1999), whereas the majority of oligodendrocytes immigrate from an extracerebellar germinal site. Our observations also show that *Ascl1* enhances the generation of interneurons from VZ progenitors, and hampers the acquisition of astroglial identities, suggesting that these two lineages may be related and that *Ascl1* biases the choices of VZ progenitors towards interneuron fates.

Role of Ascl1 in the differentiation of cerebellar inhibitory interneurons and glia

Our study shows that *Ascl1* is required for the differentiation of the proper amounts of cerebellar inhibitory interneurons, oligodendrocytes and astrocytes. The present results extend previous reports accounting for a reduction of these cell types in the cerebral cortex (Casarosa et al., 1999; Fode et al., 2000; Nieto and Guillemot, 2001; Parras et al., 2007), spinal cord (Battiste et al., 2007; Sugimori et al., 2007, 2008), diencephalon (Miyoshi et al., 2004) and olfactory bulb (Parras et al., 2004). The low numbers of interneurons and oligodendrocytes observed after ablation of *Ascl1* is consistent with a regulatory function on the balance between proliferation and differentiation of cerebellar progenitors in the prospective WM as proposed by Casarosa et al. (1999) and Lo et al. (1997). A defect in the terminal differentiation may also contribute to this effect, since Ascl1 induces panneuronal and neuronal subtype differentiation programs (Castro et al., 2006; Fode et al., 2000; Parras et al., 2002). However, this is not likely to be a major pitfall, because *Ascl1*$^{-/-}$ cerebellar transplants contained fully mature basket and stellate cells (Parvalbumin is expressed in these interneurons only at the end of their maturation; Solbach and Celio, 1991). In addition to these effects, overexpression experiments point to an active role in driving VZ progenitors towards the GABAergic interneuron lineage.

Cerebellar interneurons and oligodendrocytes arise from *Ascl1* expressing progenitors that proliferate in the postnatal WM, raising the question as to whether this gene is expressed by a common progenitor and whether it promotes both neural subtypes (Parras et al., 2004, 2007) or influences the choice between the two fates, as proposed by Petryniak et al. (2007). At birth, the oligodendrocyte and interneuron lineages are separated both in the white matter and the ventricular region of the cerebellum (Milosevic and Goldman, 2004; Zhang, and Goldman 1996a). However, it is still possible that a common ancestor is present in the VZ of the embryonic cerebellar primordium, the presumptive origin of these WM progenitors (Carletti et al., 2008; Hoshino et al., 2005). To elucidate this point, we electroporated the GFP-reporter vector to the embryonic VZ at E14.5, the time when the first proliferating

interstitial progenitors can be detected by BrdU staining (data not shown). Consistent with a previous report (Hoshino et al., 2005), we found that interneurons, as well as astrocytes, can be tracked back to the VZ, while oligodendrocytes could only be labelled when the expression vector was applied intraparenchymally, suggesting that cerebellar interneurons and oligodendrocytes have distinct origins. This conclusion was further corroborated by *Ascl1* over-expression in VZ precursors, which produced negligible effects on cerebellar oligodendrocytes.

Interestingly, both *Ascl1* overexpression at E14.5 and *Ascl1* loss of function induced significant changes in the number of cerebellar astrocytes. It is unlikely that astrocyte progenitors express *Ascl1*, since this cell type was not detected neither in a recent lineage study using a tamoxifen-inducible Cre recombination line (Kim et al., 2008) nor in our analysis of the *Ascl1::GFP* mouse. Together, these results suggest that *Ascl1*, besides inducing interneuron differentiation, inhibits astrocytic differentiation.

Ascl1 has been supposed to promote interneuron (Parras et al., 2004; 2007; Mizuguchi et al., 2006) Sugimori et al., 2007) or oligodendrocyte fate (Parras et al., 2004; 2007; Petryniak et al., 2007; Sugimori et al., 2007; 2008; Jessberger et al., 2008). Our finding of two distinct sources for oligodendrocytes and interneurons help to clarify the role of *Ascl1* in the specification of these two lineages. We show that *Ascl1* is required for the correct differentiation of both cell types, and clearly rule out a function in the differential choice between the two. On the other hand *Ascl1* strongly promotes GABAergic differentiation and suppresses astrocyte generation, suggesting a possible relation between the two latter lineages. The lack of competence of VZ progenitors to originate oligodendrocytes even after *Ascl1* overexpression is probably due to the poor expression of OPC-specifying factors such as Olig2 (Parras et al., 2007; Sugimori et al., 2007, 2008) by the time of electroporation.

Extracerebellar origin of cerebellar oligodendrocytes

Our experiments show that oligodendrocytes are already present in the cerebellar parenchyma at E14.5 but they cannot be tracked by electroporation targeted to the cerebellar VZ, at the same stage, suggesting that they derive from an alternative source. The analysis of the distribution of Olig2$^+$ cells as well as the results of transplantation experiments corroborate this conclusion indicating that the majority of cerebellar oligodendrocytes descend from foreign OPCs which colonize the cerebellar primordium during embryonic life (Fig. 7). Our study does not directly address the ventricular origin of these extrinsic oligodendrocytes. Once specified, the OPCs effectively colonize adjacent brain territories migrating through a PDGF-based expansion (van Heyningen et al., 2001). It is likely that the early cerebellar OPC derives from the closest ventricular sources in the dorsal medulla (Vallstedt et al., 2005).

Although our results point to an extracerebellar origin for most cerebellar oligodendrocytes, the analysis of E12.5 transplants shows that a small fraction of these cells also originates from the donor cerebellar tissue. It is unlikely that immigrant OPCs could reach the cerebellum earlier than E12.5. Thus, endogenous OPC progenitors may be the Olig2$^+$ cells that are transiently observed in the VZ around E13.5 (Supplementary Fig. 1A). Reynolds and colleagues (Reynolds and Wilkin, 1988) had already proposed that cerebellar OPCs derive perinatally from the superior medullary velum (SMV), an extracerebellar source at the time of their analysis. At the age of our grafts (E12.5), however, the SMV is comprised into the cerebellar territory. The anterior medial part of the cerebellar primordium which gives rise to the SMV is characterized by expression of members of the FGF8 family which locally lower BMP signalling activity (Alexandre et al., 2006; Basson et al., 2008; Louvi et al., 2003). OPCs proliferation in the dorsal neural tube is known to require lower concentrations of BMPs (Vallstedt et al., 2005). Hence, our observations suggest that reduction of BMP signalling in the SMV and anterior cerebellum may allow it to become a late source of OPCs or, more likely, a niche where the immigrating OPCs proliferate and differentiate.

In conclusion, our work outlines a new model of neuron/glia specification in the cerebellum. We show that *Ascl1* is required for the formation of the correct amount of GABAergic interneurons and oligodendrocytes and suppresses the development of astrocytes. Whereas astrocytes and interneurons both originate from the VZ, most oligodendrocytes originate from extracerebellar territories, possibly the ventral hindbrain and secondarily populate the cerebellum. *Ascl1* expression in the VZ shifts progenitor fate towards the GABAergic lineage and completely suppresses that of astrocytes. We conclude that in the cerebellum GABAergic interneurons and oligodendrocytes are not lineally related and that *Ascl1* has no role in the differential choice between these two cells types. On the other hand, it promotes the generation of GABAergic interneurons at the expenses of astrocytes (Fig. 7).

Acknowledgments

We thank Béatrice Durand and Annalisa Buffo for thoughtful discussion, Giacomo Consalez and Said Maallem for critical reading of the manuscript and Rosette Goiame for skillful technical help.

This work was supported by grants from the Association pour la Recherche sur le Cancer (ARC4972) and ANR (SWITCH) to MW. PG was supported by ARC, by Regione Piemonte fellowships and by a travel grant from *Development*.

Appendix A. Supplementary data

Supplementary data associated with this article can be found, in the online version, at doi:10.1016/j.ydbio.2009.02.008.

References

Alexandre, P., Bachy, I., Marcou, M., Wassef, M., 2006. Positive and negative regulations by FGF8 contribute to midbrain roof plate developmental plasticity. Development 133, 2905–2913.

Basson, M.A., Echevarria, D., Ahn, C., Sudarov, A., Joyner, A.L., Mason, I.J., Martinez, S., Martin, G.R., 2008. Specific regions within the embryonic midbrain and cerebellum require different levels of FGF signaling during development. Development 135, 889–898.

Battiste, J., Helms, A.W., Kim, E.J., Savage, T.K., Lagace, D.C., Mandyam, C.D., Eisch, A.J., Miyoshi, G., Johnson, J.E., 2007. Ascl1 defines sequentially generated lineage-restricted neuronal and oligodendrocyte precursor cells in the spinal cord. Development 134, 285–293.

Carletti, B., Grimaldi, P., Magrassi, L., Rossi, F., 2002. Specification of cerebellar progenitors after heterotopic–heterochronic transplantation to the embryonic cns in vivo and in vitro. J. Neurosci. 22, 7132–7146.

Carletti, B., Williams, I.M., Leto, K., Nakajima, K., Magrassi, L., Rossi, F., 2008. Time constraints and positional cues in the developing cerebellum regulate Purkinje cell placement in the cortical architecture. Dev. Biol. 317, 147–160.

Casarosa, S., Fode, C., Guillemot, F., 1999. Mash1 regulates neurogenesis in the ventral telencephalon. Development 126, 525–534.

Castro, D.S., Skowronska-Krawczyk, D., Armant, O., Donaldson, I.J., Parras, C., Hunt, C., Critchley, J.A., Nguyen, L., Gossler, A., Göttgens, B., Matter, J.M., Guillemot, F., 2006. Proneural bHLH and Brn proteins coregulate a neurogenic program through cooperative binding to a conserved DNA motif. Dev. Cell. 11, 831–844.

Cheung, M., Briscoe, J., 2003. Neural crest development is regulated by the transcription factor Sox9. Development 130, 5681–5693.

Celio, M.R., 1990. Calbindin D-28k and Parvalbumin in the rat nervous system. Neuroscience 35, 345–375.

Cohen-Tannoudji, M., Babinet, C., Wassef, M., 1994. Early determination of a mouse somatosensory cortex marker. Nature 368, 460–463.

Fode, C., Ma, Q., Casarosa, S., Ang, S.-L., Anderson, D.J., Guillemot, F., 2000. A role for neural determination genes in specifying the dorsoventral identity of telencephalic neurons. Genes Dev. 14, 67–80.

Gong, S., Zheng, C., Doughty, M.L., Losos, K., Didkovsky, N., Schambra, U.B., Nowak, N.J., Joyner, A., Leblanc, G., Hatten, M.E., Heintz, N., 2003. A gene expression atlas of the central nervous system based on bacterial artificial chromosomes. Nature 30, 917–925.

Hadjantonakis, A.K., Gertenstein, M., Ikawa, M., Okabe, M., Nagy, A., 1998. Generating green fluorescent mice by germline transmission of green fluorescent ES cells. Mech. Dev. 76, 79–90.

Hashimoto, M., Mikoshiba, K., 2004. Neuronal birthdate-specific gene transfer with adenoviral vectors. J. Neurosci. 24, 286–296.
Hoshino, M., Nakamura, S., Mori, K., Kawauchi, T., Terao, M., Nishimura, Y.V., Fukuda, A., Fuse, T., Matsuo, N., Sone, M., Watanabe, M., Bito, H., Terashima, T., Wright, C.V.E., Kawaguchi, Y., Nakao, K., Nabeshima, Y., 2005. Ptf1a, a bHLH transcriptional gene, defines gabaergic neuronal fates in cerebellum. Neuron 47, 201–213.
Jankovski, A., Rossi, F., Sotelo, C., 1996. Neuronal precursors in the postnatal mouse cerebellum are fully committed cells: evidence from heterochronic transplantations. Eur. J. Neurosci. 8, 2308–2319.
Jessberger, S., Toni, N., Clemenson Jr, G.D., Ray, J., Gage, F.H., 2008. Directed differentiation of hippocampal stem/progenitor cells in the adult brain. Nat. Neurosci. 11, 888–893.
Kim, E.J., Battiste, J., Nakagawa, Y., Johnson, J.E., 2008. Ascl1 (Mash1) lineage cells contribute to discrete cell populations in CNS architecture. Mol. Cell. Neurosci. 38, 595–606.
Lee, A., Kessler, J.D., Read, T.-A., Kaiser, C., Corbeil, D., Huttner, W.B., Johnson, J.E., Wechsler-Reya, R.J., 2005. Isolation of neural stem cells from the postnatal cerebellum. Nat. Neurosci. 8, 723–729.
Leto, K., Carletti, B., Williams, I.M., Magrassi, L., Rossi, F., 2006. Different types of cerebellar GABAergic interneurons originate from a common pool of multipotent progenitor cells. J. Neurosci. 26, 11682–11694.
Lo, L., Dormand, E., Greenwood, A., Anderson, D.J., 2002. Comparison of the generic neuronal differentiation and neuron subtype specification functions of mammalian achaete-scute and atonal homologs in cultured neural progenitor cells. Development 129, 1553–1567.
Lo, L., Sommer, L., Anderson, D.J., 1997. MASH1 maintains competence for BMP2-induced neuronal differentiation in post-migratory neural crest cells. Curr. Biol. 7, 440–450.
Louvi, A., Alexandre, P., Metin, C., Wurst, W., Wassef, M., 2003. The isthmic neuroepithelium is essential for cerebellar midline fusion. Development 130, 5319–5330.
Maricich, S.M., Herrup, K., 1999. Pax-2 expression defines a subset of GABAergic interneurons and their precursors in the developing murine cerebellum. J. Neurobiol. 41, 281–294.
Milosevic, A., Goldman, E.G., 2002. Progenitors in the postnatal cerebellar white matter are antigenically heterogeneous. J. Comp. Neurol. 452, 192–203.
Milosevic, A., Goldman, J.E., 2004. Potential of progenitors from postnatal cerebellar neuroepithelium and white matter: lineage specified vs. multipotent fate. Mol. Cell. Neurosci. 26, 342–353.
Miyoshi, G., Bessho, Y., Yamada, S., Kageyama, R., 2004. Identification of a novel basic helix–loop–helix gene, heslike, and its role in GABAergic neurogenesis. J. Neurosci. 24, 3672–3682.
Mizuguchi, R., Kriks, S., Cordes, R., Gossler, A., Ma, Q., Goulding, M., 2006. Ascl1 and Gsh1/2 control inhibitory and excitatory cell fate in spinal sensory interneurons. Nat. Neurosci. 9, 770–778.
Nieto, S.B., Guillemot, 2001. Neural bHLH genes control the neuronal versus glial fate decision in cortical progenitors. Neuron 29, 401–413.
Parras, C.M., Hunt, C., Sugimori, M., Nakafuku, M., Rowitch, D., Guillemot, F., 2007. The proneural gene mash1 specifies an early population of telencephalic oligodendrocytes. J. Neursci. 27, 4233–4242.
Parras, C.M., Schuurmans, C., Scardigli, R., Kim, J., Anderson, D.J., Guillemot, F., 2002. Divergent functions of the proneural genes Mash1 and Ngn2 in the specification of neuronal subtype identity. 16, 324–338.
Parras, G., Britz, Soares, Galichet, Battiste, Johnson, Nakafuku, Bescovi, Guillemot, 2004. Mash1 specifies neurons and oligodendrocytes in the postnatal brain. EMBO J. 23, 4495–4505.
Petryniak, M.A., Potter, G.B., Rowitch, D.H., Rubenstein, J.L.R., 2007. Dlx1 and Dlx2 Control Neuronal versus oligodendroglial cell fate acquisition in the developing forebrain. Neuron 55, 417–433.
Pfeffer, P.L., Payer, B., Reim, G., di Magliano, M.P., Busslinger, M., 2002. The activation and maintenance of Pax2 expression at the mid-hindbrain boundary is controlled by separate enhancers. Development 129, 307–318.
Reynolds, W., Wilkin, G.P., 1988. Development of macroglial cells in rat cerebellum II. An in situ immunohisotchemical study of oligodendroglial lineage from precursor to mature myelinating cell. Development 102, 409–425.
Solbach, S., Celio, M.R., 1991. Ontogeny of the calcium binding protein parvalbumin in the rat nervous system. Anat. Embryol. 184, 103–124.
Spokony, R.F., Aoki, Y., Saint-Germain, N., Magner-Fink, E., Saint-Jeannet, J.P., 2002. The transcription factor Sox9 is required for cranial neural crest development in Xenopus. Development 129, 421–432.
Stolt, C.C., Lommes, P., Sock, E., Chaboissier, M.C., Schedl, A., Wegner, M., 2003. The Sox9 transcription factor determines glial fate choice in the developing spinal cord. Genes Dev. 17, 1677–1689.
Storck, T., Schulte, S., Hofmann, K., Stoffel, W., 1992. Structure, expression, and functional analysis of a Na^+-dependent glutamate/aspartate transporter from rat brain. Proc. Natl. Acad. Sci. 89, 10955–10959.
Sugimori, M., Nagao, M., Bertrand, N., Parras, C.M., Guillemot, F., Nakafuku, M., 2007. Combinatorial actions of patterning and HLH transcription factors in the spatiotemporal control of neurogenesis and gliogenesis in the developing spinal cord. Development 134, 1617–1629.
Sugimori, M., Nagao, M., Parras, C.M., Nakatani, H., Lebel, M., Guillemot, F., Nakafuku, M., 2008. Ascl1 is required for oligodendrocyte development in the spinal cord. Development 135, 1271–1281.
Vallstedt, A., Klos, J.M., Ericson, J., 2005. Multiple dorsoventral origins of oligodendrocyte generation in the spinal cord and hindbrain. Neuron 45, 55–67.
van Heyningen, P., Calver, A.R., Richardson, W.D., 2001. Control of progenitor cell number by mitogen supply and demand. Curr. Biol. 11, 232–241.
Wassef, M., Zanetta, J.P., Brehier, A., Sotelo, C., 1985. Transient biochemical compartmentalization of Purkinje cells during early cerebellar development. Dev. Biol. 111, 129–137.
Wilkinson, D.G., 1992. In Situ Hybridization: a Practical Approach. Oxford University Press, New York.
Weisheit, G., Gliem, M., Endl, E., Pfeffer, P.L., Busslinger, M., Schilling, K., 2006. Postnatal development of the murine cerebellar cortex: formation and early dispersal of basket, stellate and Golgi neurons. Eur. J. Neurosci. 24, 466–478.
Wildner, H., Muller, T., Cho, S.-H., Brohl, D., Cepko, C.L., Guillemot, F., Birchmeier, C., 2006. dILA neurons in the dorsal spinal cord are the product of terminal and non-terminal asymmetric progenitor cell divisions, and require Mash1 for their development. Development 133, 2105–2113.
Zhang, L.G., Goldman, J.E., 1996a. Generation of cerebellar interneurons from dividing progenitors in white matter. Neuron 16, 47–54.
Zhang, L.G., Goldman, J.E., 1996b. Developmental fates and migratory pathways of dividing progenitors in the postnatal rat cerebellum. J. Comp. Neurol. 370, 536–550.
Zhou, Q., Anderson, D.J., 2002. The bHLH transcription factors OLIG2 and OLIG1 couple neuronal and glial subtype specification. Cell 109, 61–73.
Zordan, C., Hawkes, Consalez, 2008. Comparative analysis of proneural gene expression in the embryonic cerebellum. Dev. Dyn. 237, 1726–1735.